

Despite the suggestive character of these responses of the Mars sample, the environmental conditions on Mars are sufficiently different from those on Earth to require cautious interpretation. A high ultraviolet flux strikes the martian surface material, and may result in the production of highly reactive compounds capable of oxidizing the labeled nutrient. However, any explanation must account for the kinetics of the reaction as well as the heat lability of such oxidants or catalysts at 170° to 175°C. Similarly, the absorption of radioactive gas after the second injection of nutrient may be facilitated by alkalinity induced in the martian soil by wetting. An absorption of CO₂ was also seen in the GEX upon wetting the sample.

Final interpretation of the results must await the results from the investigations on the second lander, the completion of Viking 1 studies, and ground-based laboratory experiments.

HAROLD P. KLEIN
NASA Ames Research Center,
Moffett Field, California 94035

NORMAN H. HOROWITZ
Division of Biology,
California Institute of Technology,
Pasadena 91125

GILBERT V. LEVIN
Biospherics Incorporated,
Rockville, Maryland 20852

VANCE I. OYAMA
NASA Ames Research Center

JOSHUA LEDERBERG
Department of Genetics, Stanford
University, Stanford, California 94305

ALEXANDER RICH
Department of Biology,
Massachusetts Institute of Technology,
Cambridge 02139

JERRY S. HUBBARD
Department of Biology, Georgia
Institute of Technology, Atlanta 30332

GEORGE L. HOBBY
Department of Biology,
California Institute of Technology

PATRICIA A. STRAAT
Biospherics Incorporated

BONNIE J. BERDAHL
GLENN C. CARLE
NASA Ames Research Center

FREDERICK S. BROWN
TRW Systems, One Space Park,
Redondo Beach, California 90278

RICHARD D. JOHNSON
NASA Ames Research Center

References and Notes

1. N. H. Horowitz, J. S. Hubbard, G. L. Hobby, *Icarus* **16**, 147 (1972).
2. G. V. Levin, *ibid.*, p. 153.
3. V. I. Oyama, *ibid.*, p. 167.
4. H. P. Klein, *Origins Life* **5**, 431 (1974); H. P. Klein, J. Lederberg, A. Rich, N. H. Horowitz, V. I. Oyama, G. V. Levin, *Nature (London)* **262**, 24 (1976).

5. J. J. McDade, in *Planetary Quarantine: Principles, Methods, and Problems*, L. B. Hall, Ed. (Gordon & Breach, New York, 1971), pp. 37-62.
6. L. B. Hall, in *Foundations of Space Biology and Medicine*, M. Calvin and O. G. Gazenko, Eds. (Science and Technology Information Office, NASA, Washington, D.C., 1975), vol. 1, pp. 403-430.
7. Additional accounts of each of the three biological experiments are being prepared by the principal investigators and their coinvestigators: Norman H. Horowitz (pyrolytic release experiment), Gilbert V. Levin (labeled release experiment), and Vance I. Oyama (gas exchange experiment).
8. N. H. Horowitz, *Accounts Chem. Res.* **9**, 1 (1976).
9. J. S. Hubbard, J. P. Hardy, N. H. Horowitz, *Proc. Natl. Acad. Sci. U.S.A.* **68**, 474 (1971); J. S. Hubbard, J. P. Hardy, G. E. Voecks, E. E. Golub, *J. Mol. Evol.* **2**, 149 (1973); J. S. Hubbard, G. E. Voecks, G. L. Hobby, J. P. Ferris, E. A. Williams, D. E. Nicodem, *ibid.* **5**, 223 (1975).
10. J. S. Hubbard, G. L. Hobby, N. H. Horowitz, P. J. Geiger, F. A. Morelli, *Appl. Microbiol.* **19**, 32 (1970); J. S. Hubbard, *Origins Life*, in press.
11. H. Kieffer, personal communication.
12. V. I. Oyama, B. J. Berdahl, G. C. Carle, M. E. Lehwalt, H. S. Ginoza, *Origins Life*, in press; E. L. Merek and V. I. Oyama, *Life Sciences Space Res.* **8**, 108 (1970); V. I. Oyama, E. L. Merek, M. P. Silverman, C. W. Boylen, in *Proceedings of the Second Lunar Science Conference*, A. A. Levinson, Ed. (MIT Press, Cambridge, Mass., 1971), vol. 2, p. 1931; V. I. Oyama, B. J. Berdahl, C. W. Boylen, E. L. Merek, in *Third Lunar Science Conference*, C. Watkins, Ed. (Lunar Science Institute, Houston, 1972), p. 590.
13. Solid volume of soil delivered was estimated to be 0.465 cm³.
14. The composition of the mixture was 5.51 percent Kr, 2.84 percent CO₂, 91.47 percent He, 0.14 percent N₂, 0.035 percent O₂. The GEX test cell temperatures ranged from 8.3° to 10.8°C.
15. Nutrient volume injected into the test cell estimated from the quantity of Ne in the headspace above the incubating soil. Neon was added to the nutrient ampule before it was sealed.
16. H. L. Clever and R. Battino, in *Solutions and Solubilities*, M. R. J. Dack, Ed. (Wiley, New York, 1975), part 1, chap. 7; T. J. Morrison and N. B. Johnstone, *J. Chem. Soc.* (1954), p. 3441; S. Y. Yet and R. E. Peterson, *J. Pharm. Sci.* **53**, 822 (1964); J. D. Cos and A. J. Head, *Trans. Faraday Soc.* **58**, 1839 (1962); W. H. Austin, E. Lacombe, P. W. Rand, M. Chatterjee, *J. Appl. Physiol.* **18**, 301 (1963); T. J. Morrison and F. Billett, *J. Chem. Soc.* (1952), p. 3819.
17. G. V. Levin and P. A. Straat, *Origins Life*, in press.
18. G. V. Levin, *Adv. Appl. Microbiol.* **5**, 95 (1963).
19. K. Biemann, J. Oro, P. Toulmin III, L. E. Orgel, A. O. Nier, D. M. Anderson, P. G. Simmonds, D. Flory, A. V. Diaz, D. R. Rushneak, J. A. Biller, *Science*, **194**, 72 (1976).
20. N. H. Horowitz, R. E. Cameron, J. S. Hubbard, *ibid.* **176**, 242 (1972).
21. We acknowledge the effective and tireless efforts of the engineers who are part of the Viking Biology Flight team and without whom these experiments could not have been accomplished. R. I. Gilje is chief engineer on this team, which also includes S. Loer, C. Reichwein, G. Bowman, and D. Buckendahl. Supported, in part, by NASA contracts NAS1-9690 (to G.V.L.), NAS1-12311 (to N.H.H.), NAS1-13422 (to J.S.H.), and by NASA grants NGR-05002308 (to N.H.H.) and NSG-7069 (to J.S.H.). We also acknowledge the profound contribution to the Viking mission and particularly to the development of life detection concepts, of our former colleague and deputy team leader, Dr. Wolf Vishniac. His untimely accidental death in Antarctica in 1973 deprived us of his keen insight and inquiring mind at a crucial time in this study. The invaluable assistance of Dr. Richard S. Young in the preparation of this manuscript is also acknowledged.

6 September 1976

Sanidine: Predicted and Observed Monoclinic-to-Triclinic Reversible Transformations at High Pressure

Abstract. High sanidine, (K,Na)AlSi₃O₈, transforms reversibly to a triclinic phase at high pressure. This is analogous to the high-temperature monalbite transformation. Disordered alkali feldspars of various compositions have unit-cell dimensions which are very similar at the transition ($a = 8.30 \text{ \AA}$, $b = 12.97 \text{ \AA}$, $c = 7.14 \text{ \AA}$, and $\beta = 116.2^\circ$), indicating that the transformation is structurally controlled. Changes in temperature, pressure, and the sodium/potassium ratio cause similar structural variations: angles between adjacent, rigid tetrahedra vary to accommodate changing effective alkali cation sizes.

A well-known high-temperature phase transformation is that of disordered monoclinic albite (monalbite, NaAlSi₃O₈), which becomes triclinic (high albite) at temperatures below $\approx 1100^\circ\text{C}$ because of collapse of the Al-Si framework about the alkali site (1, vol. 1; 2). The transformation temperature decreases with increasing K/Na ratio, and at room conditions metastable disordered alkali feldspars more potassic than $\approx \text{Or}_{38}$ (3) are monoclinic high sanidines (4). Mineral crystal structures vary continuously with changes in pressure as well as temperature, and in many silicates the changes during compression to high pressure are similar to changes during cooling from high temperatures (5). On this basis it was predicted that high sanidine would transform to the triclinic high-albite structure at elevated pressures,

with more potassic sanidines requiring higher pressures. This prediction has now been confirmed, and the monoclinic-to-triclinic transition has been observed in two high sanidines: Or₆₇ at $12 \pm 1 \text{ kbar}$ and Or₈₂ at $18 \pm 1 \text{ kbar}$.

Single crystals of high sanidine were selected from material described by MacKenzie (6). Eifel sanidine from Wehr and Eifel (Or₈₂Ab₁₇An₁) and Mineral Creek sanidine from San Juan, Colorado (Larsen 10; Or₆₇Ab₃₁An₂), were the specimens used. Crystals were mounted with a gillespite reference crystal in a miniature diamond pressure cell (7), using the Van Valkenburg metal-foil gasketing technique. Index-of-refraction oil was the hydrostatic pressure medium. Unit-cell dimensions were measured at several pressures to 38 kbar using single-

crystal x-ray photographic techniques. Pressure was calibrated from the known volume compressibility of alkali feldspar (1, vol. 2) and from the 26-kbar red-to-blue gillespite transformation (8).

Monoclinic unit-cell parameters vary regularly with increasing pressure; a , b , and c decrease, while β increases slightly (see Fig. 1). At sufficient pressure high-sandine cell dimensions reach "critical values" of $a = 8.30 \text{ \AA}$, $b = 12.97 \text{ \AA}$, $c = 7.14 \text{ \AA}$, and $\beta = 116.2^\circ$. At higher pressures α and γ deviate from 90° , in-

dicating a transition to triclinic symmetry (see Fig. 1). Comparison of critical cell dimensions with those of monalbite at 1100°C [$a = 8.28 \text{ \AA}$, $b = 12.96 \text{ \AA}$, $c = 7.15 \text{ \AA}$, and $\beta = 116.1^\circ$ (2)] and of Or_{38} at room conditions [$a = 8.32 \text{ \AA}$, $b = 12.96 \text{ \AA}$, $c = 7.15 \text{ \AA}$, and $\beta = 116.2^\circ$ (1, vol. 1)] reveals that the monoclinic-to-triclinic transition is structurally controlled, since cell dimensions are nearly constant along the pressure-composition (P - X) and temperature-composition (T - X) transition curves. The

monalbite-to-high albite transition has usually been described as the result of "collapse" of the Al-Si framework about an alkali site which is too small to support a framework with monoclinic symmetry. The size of individual tetrahedra does not change appreciably with temperature or pressure (9), but the alkali site may change size in three ways, by changing temperature, pressure, or Na/K ratio. When the effective size of the alkali site falls below the critical level (either by cooling or compression or Na substitution) the monoclinic framework will distort to triclinic symmetry.

Since changes in temperature, pressure, and Na/K ratio seem to cause similar structural responses, it appears reasonable to postulate a transition surface in P - T - X space which approximates a surface of constant structure for disordered alkali feldspars (see Fig. 2). The cell dimensions are observed to be constant on the T - X and P - X faces of Fig. 2, but it should be emphasized that no data are available on the central portion of Fig. 2, and a planar surface has been assumed.

In reversible phase transformations involving a reduction of symmetry twinning may occur. The twin law will be a symmetry element of the higher-symmetry form, and the twin will result from simultaneous nucleation of two different, but symmetrically related, orientations of the low-symmetry form. In the transition from monalbite to high albite ($C2/m \rightarrow C\bar{1}$) two types of twins are common: the albite and pericline laws. In Or_{67} no twinning was observed above 12 kbar, but Or_{82} did twin on the albite law above 18 kbar. It is expected that pericline twins could also occur, and that the types and extent of twinning will depend, in part, on crystal defects and morphology.

The geothermal gradient of the crust averages $\approx 15^\circ\text{C}$ per kilometer, or 45°C per kilobar, assuming 1 kbar per 3.0 km (10). The slope of the transition surface (Fig. 2) in the P - T section is somewhat steeper ($\approx 70^\circ\text{C}$ per kilobar). Therefore, some alkali feldspars which are monoclinic at surface conditions may have been triclinic at depth, especially if local thermal gradients are low. On the other hand, volcanic sanidines which have not been reburied were probably monoclinic throughout their histories. Since the monoclinic-to-triclinic transition is displacive (and probably second-order) there will be no obvious evidence of triclinic history in disordered monoclinic alkali feldspars. Unlike the slow ordering and exsolution transitions in feldspars, the reversible high-pressure transition is

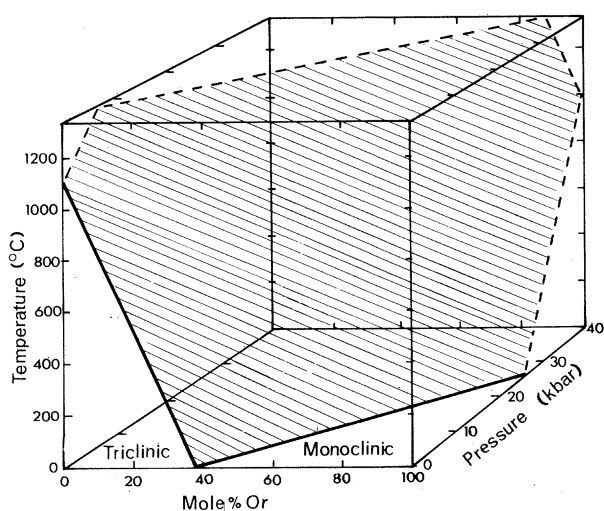
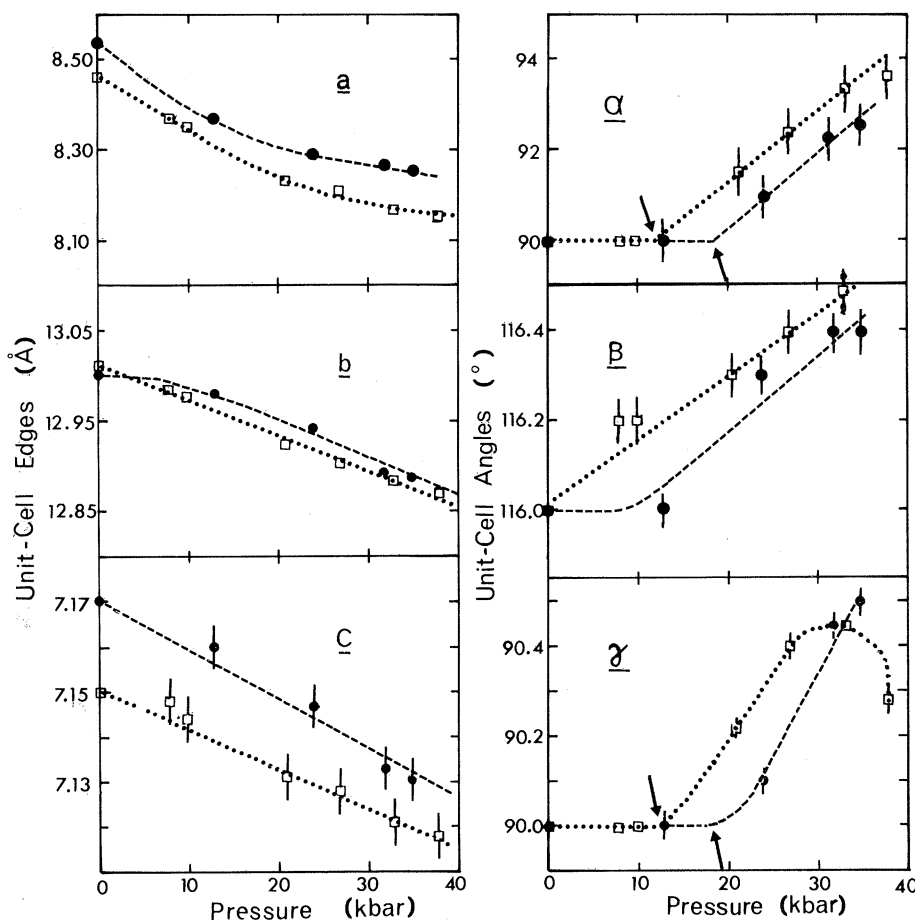


Fig. 1 (above). Unit-cell dimensions of high sanidines as a function of pressure. Angles α and γ deviate from 90° at 12 ± 1 kbar for Or_{67} (squares) and at 18 ± 1 kbar for Or_{82} (circles), indicating triclinic symmetry. Arrows indicate suggested transition points. Fig. 2 (left). Monoclinic-to-triclinic transition surface for disordered alkali feldspars. Since unit-cell dimensions are constant along the T - X and P - X curves of this surface, the surface may also represent an isostructural region.

of no help in determining the thermal or pressure history of a feldspar-bearing rock. However, it is possible that the pressure-induced monoclinic-to-triclinic transition interacts with the order-induced monoclinic-to-triclinic (orthoclase-to-microcline) transition. In this event pressure would enhance the formation of the triclinic ordered form. Furthermore, it is anticipated that partially ordered monoclinic feldspars will transform to triclinic symmetry at lower pressures than disordered feldspars of the same composition.

Perhaps the most intriguing aspect of this work is the evidence of possible isostructural *P-T-X* surfaces, and their close relationships to phase transition surfaces. The stability of many minerals is limited by geometrical packing limits of adjacent groups of polyhedra (such as micas, pyroxenes, amphiboles, and olivines). Since changes in temperature, pressure, and composition may all have the same effect of varying polyhedral size ratios (9), the concept of isostructural stability fields in *P-T-X* space does not seem unreasonable for these minerals. Of course, other phase regions will intersect the geometrically limiting surface. Still, the existence of isostructural *P-T-X* surfaces, and their close relationship to phase transition surfaces, may allow prediction of some phase equilibria from basic structural data.

ROBERT M. HAZEN*

Department of Mineralogy and Petrology, University of Cambridge, Cambridge CB2 3EW, England

References and Notes

1. J. V. Smith, *Feldspar Minerals* (Springer-Verlag, New York, 1974).
2. C. T. Prewitt, *Am. Mineral.*, in press.
3. Natural feldspars consist predominantly of three components: NaAlSi₃O₈ (albite), KAlSi₃O₈ (K-feldspar), and CaAl₂Si₂O₈ (anorthite). The composition of a given specimen is usually abbreviated Or_xAb_yAn_z, where *x*, *y*, and *z* give the mole percentages of the K-feldspar, albite, and anorthite components, respectively. In this report the use of Or_x alone implies the approximate composition Or_xAb_{1-x}.
4. Disordered feldspars at room temperature are metastable. Slow-cooled feldspars possess ordered Al-Si arrangements, while intermediate K/Na feldspars have the additional complication of exsolution of Na- and K-rich lamellae. High sanidines, in which there is complete Al-Si disorder and no exsolution, come from rapidly chilled volcanic rocks.
5. R. M. Hazen, thesis, Harvard University (1975).
6. W. MacKenzie, *Am. J. Sci.*, Bowen Volume, 319 (1952).
7. L. Merrill and W. A. Bassett, *Rev. Sci. Instrum.* 45, 290 (1974).
8. R. M. Hazen and C. W. Burnham, *Am. Mineral.* 59, 1166 (1974).
9. R. M. Hazen and C. T. Prewitt, in preparation.
10. P. J. Wyllie, *The Dynamic Earth* (Wiley, New York, 1971).
11. I thank J. D. C. McConnell, S. Agrell, A. Putnis, and C. T. Prewitt for their thoughtful reviews of the manuscript. Supported by a NATO Postdoctoral Fellowship in Science.

* Present address: Geophysical Laboratory, Carnegie Institution of Washington, 2801 Upton Street, NW, Washington, D.C. 20008.

16 June 1976; revised 23 July 1976

Jupiter's Spectrum Between 12 and 24 Micrometers

Abstract. Spectroscopic measurements of the thermal radiation from Jupiter between 12 and 24 micrometers (420 to 840 reciprocal centimeters) with a resolution of 4 reciprocal centimeters are used to infer the Jovian temperature structure in the pressure region 0.1 to 0.4 atmosphere. The brightness temperature spectrum is in good agreement with previous ground-based measurements between 11 and 13 micrometers and with airborne measurements between 18 and 25 micrometers. However, the integrated flux calculated for a filter window and viewing angle equivalent to those of the 20 micrometer channel of Pioneer 10 is 20 percent below that measured by the Pioneer infrared radiometer. The Q branch of the ν_5 fundamental band of acetylene at 730 reciprocal centimeters appears in emission and leads to a mixing ratio estimate of $10^{-6 \pm 0.5}$.

The spectrum of Jupiter between 12 and 24 μm is dominated by the *S*(1) rotational line of the collisionally induced H₂ dipole, with a maximum opacity near 17 μm . We have observed Jupiter in this spectral region on 15 and 23 October 1975, using the 91-cm telescope of the G. P. Kuiper Airborne C141 Observatory operated at an altitude of 12,000 m. At this altitude the amount of CO₂ in the line of sight is reduced by nearly a factor of 7 compared to that at ground-based sites and, except for the region 14.3 to 15.9 μm , the brightness temperature spectrum of the region containing the center and the high- and low-frequency wings of the *S*(1) line can be obtained with a single instrument. For wavelengths $\lambda < 13.8 \mu\text{m}$, ground-based measurements have been made by Gillett *et al.* (1) and Gillett (2) with a resolution of $\Delta\lambda/\lambda = 0.015$, by Aitken and Jones (3) with $\Delta\lambda/\lambda = 0.007$, by Ridgway (4) and Combes *et al.* (5) with a resolution of 1.3 cm^{-1} ($\Delta\lambda/\lambda \sim 0.0018$). For $\lambda > 18 \mu\text{m}$, aircraft measurements with $\Delta\lambda/\lambda = 0.03$ have been published by Houck *et al.* (6). In addition, the Pioneer 10 infrared radiometer has made broad-band (16 to 24 μm) radiance measurements from an aspect similar to that viewed from the earth, reported by Ingersoll *et al.* (7).

Our observations were made with a stepping Michelson interferometer using a KBr beam splitter and a Ge:Ga bolometer detector operated at 2°K. The instrument field of view was 36 arc seconds, while Jupiter subtended a mean diameter of 46 arc seconds. Telescope and sky background were canceled by oscillating the telescope secondary mirror between Jupiter and a point on the sky 3 arc minutes away at a rate of 28 hertz. The integrated signal from the residual background was less than 2 percent of the signal from Jupiter. Three spectra with a resolution of 1.95 cm^{-1} and nine spectra with a resolution of 3.9 cm^{-1} were obtained.

For absolute calibration, observations were made near the lunar limb ($53^\circ \pm 5^\circ\text{N}$, $20^\circ \pm 8^\circ\text{W}$) in the vicinity of

the crater Aristarchus, located in the northwest quadrant of Oceanus Procellarum. The solar meridian at the time of the observation was 49°W . For the emissivity and the temperature we have adopted $\epsilon = 0.90 \pm 0.05$ and $T = 394^\circ \pm 7^\circ\text{K}$, respectively, in the wavelength range of interest. The emissivity is based on a number of observations summarized by Linsky (8); the temperature was deduced from Apollo 17 observations by Low and Mendell (9), Apollo 17 heat flow experiments by Keihm and Langseth (10), and theoretical thermal response models by Schloerb and Muhleman (11).

Since here we are mainly concerned with the accurate definition of the continuum absolute brightness temperature spectrum, we present in the following the results of the analysis of the spectra obtained with a resolution of $\sim 4 \text{cm}^{-1}$. A more detailed description of the instrumentation, calibration methods, and analysis of the 2- cm^{-1} spectra will be presented elsewhere (12). The center line in Fig. 1 shows the calculated spectral brightness temperature of Jupiter (average of nine 4- cm^{-1} spectra, each requiring approximately 6 minutes of integration time) based on the lunar ratio spectrum, with $T_{\text{moon}} = 394^\circ\text{K}$ and $\epsilon_{\text{moon}} = 0.90$. No data are shown below 400 cm^{-1} , between 640 and 700 cm^{-1} , and above 850 cm^{-1} , where the combined system and atmospheric transmission drops below 20 percent of its maximum value. The brightness temperature increases at frequencies above and below the center of the *S*(1) line at 587 cm^{-1} , indicating a rising temperature with depth, except for frequencies below 450 cm^{-1} , where the influence of the *S*(0) rotational line near 350 cm^{-1} is observed. The relatively constant brightness temperature between 560 and 640 cm^{-1} , a region where the opacity significantly increases toward 600 cm^{-1} , indicates the presence of a level where the temperature is constant or increases with height.

The center line in Fig. 1 is bounded by the spectra representing ± 1 standard de-